Potent New Antiviral Compound Shows Similar Inhibition and Structural Interactions with Drug Resistant Mutants and Wild Type HIV-1 Protease†

Yuan-Fang Wang,‡ Yunfeng Tie,‡ Peter I. Boross,‡,§ Jozsef Tozser,§ Arun K. Ghosh,|| Robert W. Harrison,⊥ and Irene T. Weber*,‡,#

Department of Biology, Molecular Basis of Disease, Georgia State University, Atlanta, Georgia 30303, Department of Chemistry, Molecular Basis of Disease, Georgia State University, Atlanta, Georgia 30303, Department of Biochemistry and Molecular Biology, Faculty of Medicine, University of Debrecen, Debrecen, Hungary, Department of Chemistry and Medicinal Chemistry, Purdue University, West Lafayette, Indiana 47907, and Department of Computer Science, Georgia State University, Atlanta, Georgia 30303

Received April 24, 2007

The potent new antiviral inhibitor GRL-98065 (**1**) of HIV-1 protease (PR) has been studied with PR variants containing the single mutations D30N, I50V, V82A, and I84V that provide resistance to the major clinical inhibitors. Compound **1** had inhibition constants of 17-fold, 8-fold, 3-fold, and 3-fold, respectively, for PR_{D30N}, PR_{I50V}, PR_{V82A}, and PR_{I84V} relative to wild type PR. The chemically related darunavir had similar relative inhibition, except for PR_{D30N}, where inhibitor **1** was approximately 3-fold less potent. The high resolution (1.11−1.60 Å) crystal structures of PR mutant complexes with inhibitor **1** showed small changes relative to the wild type enzyme. PR_{D30N} and PR_{V82A} showed compensating interactions with inhibitor **1** relative to those of PR, while reduced hydrophobic contacts were observed with PR_{I50V} and PR_{I84V}. Importantly, inhibitor **1** complexes showed fewer changes relative to wild type enzyme than reported for darunavir complexes. Therefore, inhibitor **1** is a valuable addition to the antiviral inhibitors with high potency against resistant strains of HIV.

Introduction

Highly active antiretroviral therapy (HAART[a]), consisting of a combination of drugs that inhibit the HIV-1 protease (PR) or the reverse transcriptase, has provided an effective treatment for AIDS.[1−3] However, the success of long-term therapy is limited by the rapid emergence of drug resistance.[4] Resistance to antiviral PR inhibitors arises by distinct mutations in the PR gene.[5−7] Many of these mutations provide resistance by altering the amino acid residues forming the inhibitor binding site of the PR and, thus, reducing the affinity for the inhibitor. Most of the current drugs show significantly reduced inhibition of PR with such resistant mutations. Therefore, new antiviral inhibitors are being developed.[8] One successful approach is to design inhibitors that provide more interactions with the main chain atoms of PR.[9] These interactions cannot easily be changed by mutation. Such new nonpeptide inhibitors, like the recently FDA-approved darunavir (TMC-114), have already demonstrated success in clinical trials in treating infections with resistant virus.

PR mutations observed in resistant HIV include D30N, I50V, V82A, and I84V, which individually provide high levels of resistance to the major clinical inhibitors. These four mutations alter residues forming the binding site for peptide substrates or inhibitors. Previously, we have analyzed the effect of darunavir on the structure and inhibition of PR with each of these mutations.[10,11] Darunavir showed lower affinity for PR with the D30N and I50V mutations. The mutation D30N, which removes the negative charge of the amino acid side chain, is selected frequently in clinical isolates on exposure to nelfinavir.[12] PR_{D30N} showed altered activity for different substrates compared to wild type PR.[13] Crystal structures of PR_{D30N} with different inhibitors have shown changes in the position of the side chain of residue 30.[10,14] Asp30 forms hydrogen bond interactions with the aniline group of darunavir. In the D30N mutant, these direct interactions were replaced by a weaker water-mediated hydrogen bond interaction, in agreement with the 30-fold weaker inhibition of darunavir for PR_{D30N} compared to wild type PR. Mutation I50V is very common on exposure to amprenavir,[15] the drug that is chemically most related to darunavir. I50V also confers resistance to darunavir.[16] Our structural analysis showed that PR_{I50V} has reduced interactions with the aniline group of darunavir consistent with a 9-fold worse inhibition. Mutations V82A and I84V are observed with all the clinical inhibitors.[7] These mutations had smaller structural changes in the interactions with darunavir and little change in the inhibition relative to wild type PR.

Compound **1** [(1*R*,5*S*,6*R*)-2,8-dioxabicyclo[3.3.0]oct-6-yl] *N*-[(2S,3R)-4-[(3,4-methylenedioxyphenyl)sulfonyl-(2-methylpropyl)amino]-3-hydroxy-1-phenyl-butan-2-yl] carbamate (Figure 1) is a potent new antiviral inhibitor derived from darunavir in which the aniline group has been replaced by a 1,3-benzodioxole group.[9,17] This chemical change is expected to alter the affinity of the compound, especially for mutants PR_{D30N} and PR_{I50V}, because the aniline group of darunavir interacts with Asp30 and Ile50. However, crystal structures show that many of the HIV PR interactions are similar for inhibitor **1** and darunavir.[17] The antiviral data show that inhibitor **1** is highly potent against HIV-infected cells with IC_{50} values of 0.2−0.5 nM compared to 3 nM for darunavir and has minimal cytotox-

† PDB IDs: 2Z4O for PR/inhibitor **1**, 2QD7 for PR_{V82A}/inhibitor **1**, 2QD8 for PR_{I84V}/inhibitor **1**, 2QCI for PR_{D30N}/inhibitor **1**, and 2QD6 for PR_{I50V}/inhibitor **1**.

* To whom correspondence should be addressed. Department of Biology, Georgia State University, 402 Kell Hall, 24 Peachtree Center Ave., Atlanta GA 30303. Phone: 404-413-5411. Fax: 404-413-5301. E-mail: iweber@gsu.edu.

‡ Department of Biology, Georgia State University.

§ Department of Biochemistry and Molecular Biology, University of Debrecen.

|| Department of Chemistry and Medicinal Chemistry, Purdue University.

⊥ Department of Computer Science, Georgia State University.

Department of Chemistry, Georgia State University.

[a] Abbreviations: PR, protease; HIV-1, human immunodeficiency virus type 1; HAART, highly active antiretroviral therapy; AIDS, acquired immunodeficiency syndrome; PI, protease inhibitor; THF, tetrahydrofuran.

10.1021/jm070482q CCC: $37.00
Published on Web 08/16/2007

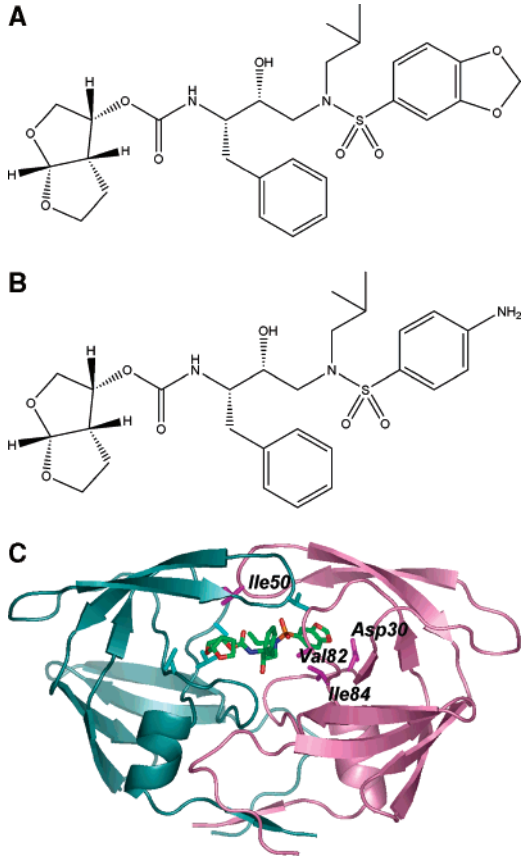

Figure 1. Structures of (A) inhibitor **1** (GRL-98065), (B) darunavir (TMC-114), and (C) PR dimer indicating location of mutations. The backbone of one subunit is shown as pink ribbons, with the sites of mutation (D30N, I50V, V82A, and I84V) indicated by magenta side chains, while the other subunit is colored in light cyan with mutation sites in darker cyan. Only one subunit is labeled. Inhibitor **1** is colored by atom type.

Table 1. Inhibition Data

protease	K_i (nM) (relative) inhibitor **1**	K_i (nM) (relative) darunavir
PR	0.27 ± 0.06 (1)	0.34 ± 0.08 (1)
PR_{D30N}	4.6 ± 0.7 (17)	1.9 ± 0.3 (5.5)
PR_{I50V}	2.1 ± 0.4 (8)	1.3 ± 0.3 (3.9)
PR_{V82A}	0.80 ± 0.06 (3)	0.54 ± 0.04 (1.6)
PR_{I84V}	0.85 ± 0.15 (3.2)	0.56 ± 0.10 (1.7)

icity.[9,17] Here, the structures and in vitro inhibition data are reported for inhibitor **1** and PR variants with the single substitutions D30N, I50V, V82A, and I84V. Inhibitor **1** and darunavir showed very similar *in vitro* inhibition of PR, PR_{V82A}, and PR_{I84V} and slightly worse inhibition of PR_{D30N} and PR_{I50V} relative to PR. Therefore, inhibitor **1** is likely to be as effective as darunavir in treating many resistant variants of HIV.

Results

Inhibition of HIV PR and the Mutants PR_{V82A}, PR_{I84V}, PR_{D30N}, and PR_{I50V} by Inhibitor 1. The inhibition constants of inhibitor **1** against PR and the drug-resistant mutants PR_{D30N}, PR_{I50V}, PR_{V82A}, and PR_{I84V} were measured using the fluorescence substrate RE(Edans)SQNY*PIVRK(Dabcyl)R,[18] an analog of the MA−CA cleavage site in the Gag-Pol polyprotein. The kinetic parameters of these mutants for hydrolysis of the fluorescence substrate have been reported in ref 10. As shown in Table 1, wild type PR had an essentially identical inhibition constant of 0.3 nM for inhibitor **1** and darunavir. Moreover, inhibitor **1** and darunavir had similar relative inhibition of 1.6- to 3-fold for PR_{V82A} and PR_{I84V} relative to PR. PR_{D30N} and PR_{I50V} had higher K_i values of 17- and 8-fold relative to PR for inhibitor **1**, compared with 6-fold and 4-fold for darunavir. Inhibitor **1** and darunavir showed the same order of relative inhibition of PR > PR_{V82A} ∼ PR_{I84V} > PR_{I50V} > PR_{D30N}.

Description of the High-Resolution Crystal Structures. The crystal structures of the drug-resistant mutants PR_{D30N}, PR_{I50V}, PR_{V82A}, and PR_{I84V} have been determined in their complexes with the new antiviral inhibitor **1** at resolutions of 1.11−1.35 Å (Figure 1). The crystallographic statistics are summarized in Table 2. The wild type PR complex was described briefly in ref 17. Each crystallographic asymmetric unit contains a dimer with the residues numbered 1−99 and 1′−99′. Three structures were determined in the space group $P2_12_12$ and the PR_{V82A} complex was solved in the $P2_12_12_1$ space group. The structures were refined to *R*-factors of 0.13−0.16, including solvent molecules, anisotropic *B*-factors, and hydrogen atoms. These high-resolution crystal structures showed clear electron density for all the protease atoms, the inhibitor, and the solvent molecules. Overall, the mutant structures were very similar to the wild type complex, with rms deviations of 0.21−0.22 Å for the main atoms of the structures in the same space group ($P2_12_12$), and 0.63 Å for the PR_{V82A}/inhibitor **1** complex in the space group $P2_12_12_1$, due to the differences in lattice packing in the two space groups.

The average *B*-factors were low for protein and inhibitor atoms. The higher resolution structures showed lower average *B*-factors. In particular, the PR_{V82A} complex had the lowest *B*-factors for protein main-chain and side-chain atoms of 7.9 Å^2 and 11.6 Å^2, respectively, compared to the values of about 15 Å^2 to 20 Å^2 for the other structures. The inhibitor atoms also showed the lowest average *B*-factors for the PR_{V82A} complex: 7.2 Å^2 compared to 11.7−12.3 Å^2 for the others. The average *B*-factors of the solvent molecules depend on the quality of the data as well as the number of solvent molecules included in refinement. The higher resolution data also provide better quality electron density maps in which more ordered solvent molecules are visible. The solvent atoms for the complexes with PR_{I50V} and PR_{V82A} showed lower average *B*-factors of 17.1 Å^2 and 19.3 Å^2, respectively, compared to 27.4−35.0 Å^2 for the other structures.

Residues with Alternate Conformations. Alternate conformations were observed in all the crystal structures. Inhibitor **1** was bound in two conformations in all structures in the space group $P2_12_12$ with relative occupancy of 0.6/0.4, although it had a single conformation in the PR_{V82A} complex in space group $P2_12_12_1$ (Figure 2). Alternate conformations were observed for the main chain atoms of residues 3−5 in PR_{V82A}, as noted previously in complexes PR_{V82A}/darunavir [PDB code 2IDW][11] and PR/JE-2147 [PDB code 1KZK].[19] There were 23 residues with two alternate conformations modeled for the side chains in PR, 23 for mutant PR_{D30N}, 29 for PR_{I50V}, 22 for PR_{V82A}, and 25 for PR_{I84V}. A similar pattern of the residues with alternate conformations was observed for the four structures (PR, PR_{I84V}, PR_{D30N}, and PR_{I50V}) in the same space group. Surface residues, especially charged residues with longer side-chains, such as arginine and lysine, showed more flexibility and were observed with more alternate conformations. However, several internal hydrophobic residues, such as Leu23, Ile33′, and Leu97/97′, had two alternate conformations. The side-chains of several residues located close to the inhibitor, Arg8, Asp30, Ile50, Pro81, Val82, and Ile84, showed alternate conformations in at least one subunit, as reported for darunavir complexes.[11]

Table 2. Data Collection and Refinement Statistics

	PR_{D30N}	PR_{I50V}	PR_{V82A}	PR_{I84V}
space group	$P2_12_12$	$P2_12_12$	$P2_12_12_1$	$P2_12_12$
	Unit Cell Dimensions: (Å)			
a	58.42	58.29	50.88	58.42
b	86.23	86.23	58.15	86.18
c	46.01	46.01	62.11	45.99
resolution range (Å)	50−1.20	50−1.28	50−1.11	50−1.35
unique reflections	73,411	60,638	73,051	51,903
R_{merge} (%) overall (final shell)	8.9 (36.8)	7.7 (41.1)	8.6 (23.0)	5.1 (30.8)
$I/\sigma(I)$ overall (final shell)	14.7 (2.3)	11.9 (2.2)	18.2 (4.0)	17.3 (4.7)
completeness (%) overall (final shell)	89.0 (51.0)	89.5 (59.3)	97.4 (80.3)	98.5 (86.6)
data range for refinement (Å)	10−1.20	10−1.28	10−1.11	10−1.35
R (%)	16.1	15.8	13.0	13.3
R_{free} (%)	19.5	20.2	16.3	17.5
No. of solvent atoms (total occupancies)	161.4	136.3	186.3	192.8
	RMS Deviation from Ideality			
bonds (Å)	0.013	0.012	0.015	0.012
angle distance (Å)	0.034	0.031	0.033	0.032
average *B*-factors (Å^2)				
main-chain atoms	15.4	15.1	7.9	14.7
side-chain atoms	20.1	19.2	11.6	18.6
inhibitor	11.8	12.3	7.2	11.3
solvent	35.0	17.1	19.3	27.4
residual density (max/min) (eÅ^{-3})	0.41/−0.33	0.39/−0.32	0.65/−0.43	0.41/−0.32
relative occupancy of inhibitor **1**	0.6/0.4	0.6/0.4	1.0	0.6/0.4

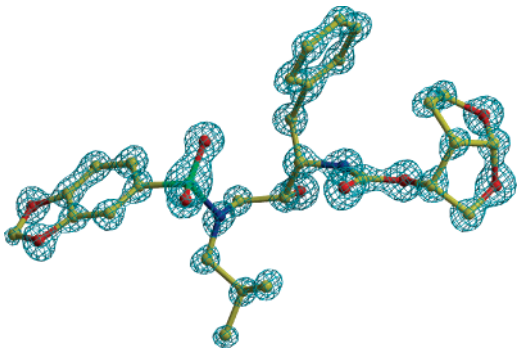

Figure 2. Electron density map for inhibitor **1** in complex with PR_{V82A}. The omit F_o-F_c map, using F_c calculated without inhibitor **1**, is contoured at 8.5σ level. Inhibitor **1** had a single conformation.

Alternate conformations were observed at the sites of mutation in most structures, except for PR_{V82A}, which had a single conformation for residues 30, 50, 82, and 84 in both subunits. The side chain of residue 30 had alternate conformations in the structures of PR_{D30N} and PR_{I50V}. The side chain of Val 82 had alternate conformations in both subunits of all structures, except for PR_{V82A}. The side chain of Ile 84 had alternate conformations in the structure of PR_{I50V}, while Ile/Val 84′ had alternate conformations in all structures, except for PR_{V82A}. The main chain atoms of residues 50 and 50′ had alternate conformations in four structures, while the side chain of Ile 50′ had alternate conformations in the PR_{I84V} structure.

Solvent Molecules in the Crystals. The high quality of the diffraction data for the structures allowed the modeling of many solvent molecules. The structures were modeled with more than 130 water molecules, ions, and other small molecules from the crystallization solutions, including many with partial occupancy, depending on the shape of the electron density and the interactions with other molecules. Sodium, chloride, and acetate ions were modeled in PR, PR_{I84V}, PR_{D30N}, and PR_{I50V} complexes, while phosphate, glycerol, and DMSO molecules were fitted to density in the PR_{V82A} structure. The sodium ion was identified for the first time in the PR and PR_{I84V} complexes with darunavir[11] and illustrated in ref 10, although there was strong evidence in other published structures that some water molecules should be identified as Na^+ (such as PDB code 1KZK, 1SDT, and 1SDV). The sodium ion was recognized initially by the abnormally low *B*-factor and positive peak when water was refined at that site and then confirmed by the six octahedral oxygen donors at the mean distance of 2.42 Å. Valence calculations suggested that the atom was either a sodium or calcium ion,[20] and only sodium was present in the crystallization conditions. The PR, PR_{D30N}, PR_{I50V}, and PR_{I84V} structures in space group $P2_12_12$ each contain one sodium ion.

HIV-1 Protease Interactions with Inhibitor 1. The numerous protease−inhibitor interactions include strong hydrogen bonds, weaker C−H···O contacts, C−H···π contacts, and the weakest van der Waals contacts, such as C−H···H−C, as described for darunavir complexes.[21] Polar interactions are important for ligand binding to the PR. Ten direct hydrogen bonds, three water-mediated hydrogen bond interactions, and five C−H···O interactions with main chain atoms were observed between the major conformation of inhibitor **1** and the PR (Figure 3A). The inhibitor hydroxyl group formed hydrogen bonds with all four carboxylate oxygens of the catalytic Asp 25 and 25′ with distances of 2.7, 2.4, 3.2, and 2.8 Å, which is likely to mimic the interactions of the tetrahedral transition state of the proteolytic reaction. At one end of the inhibitor, the two oxygen atoms of the bis-THF group formed three hydrogen bonds with the main-chain amides of Asp 29′ and Asp 30′, and there is a C−H···O interaction with Gly 48′. At the other end of the inhibitor, one of the two oxygen atoms in the 1,3-benzodioxole group interacted with the main-chain amide and the side-chain carboxylate oxygen of Asp 30. The polar interaction with the carboxylate side chain of Asp 30 appeared to be similar to the proton-mediated interaction observed between the carboxylate side chains of Asp 30 and Glu at *P*2′ in peptide analogs.[14] The other oxygen atom of the 1,3-benzodioxole group showed a water-mediated interaction with the amide of Gly 48 in the flap. The 1,3-benzodioxole group had a C−H···O interaction with Gly 48, C−H···π contacts with Ala 28, Val 32, and Ile 50′, and a water-mediated interaction with amide of Asp 29. The *P*1′ side chain had a C−H···O interaction with the carbonyl oxygen of Gly 27, while the nitrogen next to the *P*1 phenyl group of the inhibitor formed a

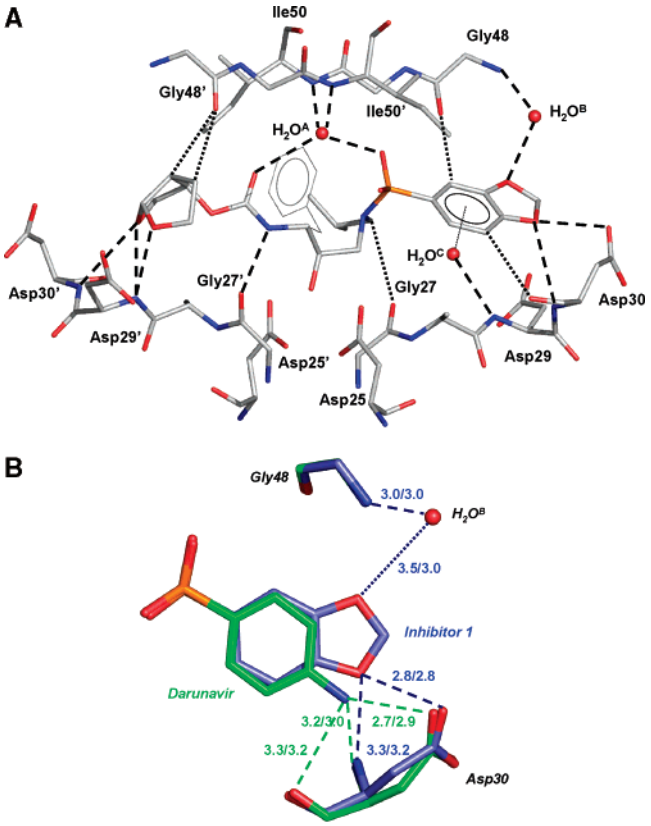

Figure 3. Protease interactions with inhibitor **1** and darunavir (A). Polar interactions of inhibitor **1** with PR The major conformation of inhibitor **1** is shown with interacting PR residues. Water is shown as red spheres. Hydrogen bond interactions are indicated by dashed lines and CH···O interactions with main chain PR atoms by dotted lines. The H_2O^C O−H···π interaction with the *P*2′ aromatic ring is shown as a gray dotted line. The interactions of the alternate conformation of inhibitor are essentially the same. (B) Comparison of PR interactions with inhibitor **1** and darunavir. Carbon atoms in PR/inhibitor **1** are colored in blue and those in PR/darunavir are green. The hydrogen bond interactions are indicated by the dashed lines, with distances in Å for the major/minor conformation of inhibitor, and colored blue for PR/inhibitor **1** and green for PR/darunavir. The dotted line indicates the water-mediated interaction with a weaker hydrogen bond for the major conformation.

hydrogen bond with the carbonyl oxygen of Gly 27′. The phenyl group has C−H···π contacts with Pro 81, Val 82, and Gly 49′. The flexible PR flaps were stabilized by the C−H···O interactions of Gly 48 and 48′ with the inhibitor. A water molecule (H_2O^A) linked the amides of Ile 50 and 50′ in the flaps with the carbonyl oxygen and one of the sulfonamide oxygen atoms of inhibitor **1**. This water is conserved in all structures of PR with inhibitors/substrates,[22] except for those urea-based inhibitors designed explicitly to substitute for this water.[23−25] Equivalent hydrogen bond interactions were observed for the minor conformation of the inhibitor except for one water-mediated hydrogen bond. The water H_2O^B formed interactions connecting oxygen in the 1,3-benzodioxole group of inhibitor **1** with the amide of Gly 48′. This hydrogen bond was longer and, therefore, weaker for the major conformation of the inhibitor (3.5 Å) than for the minor one (3.0 Å). Also, the minor conformation of inhibitor **1** formed additional C−H···π contacts between the phenyl group and Leu 23′ and Ile 84′ compared to those of the major conformation.

Comparison of the PR Interactions with Inhibitor 1 and Darunavir. It is important to compare the details of the PR interactions with inhibitor **1** to those of the chemically related darunavir. The chemical difference is that the *P*2′ aniline group of darunavir has been replaced by the 1,3-benzodioxole group in inhibitor **1** (Figure 1). The atoms of the two inhibitors (excluding the different *P*2′ groups) superimpose with a rmsd of 0.16 Å for the major conformation and 0.23 Å for the minor conformation. Therefore, the inhibitor structures are very similar for the equivalent atoms. Inhibitor **1** and darunavir formed very similar hydrogen bond, C−H···O, and C−H···π interactions with the PR; the interatomic distances are almost identical. However, the interactions of the chemically distinct *P*2′ groups differ as shown in Figure 3B. The three direct hydrogen bonds formed by the aniline group of darunavir to Asp 30 were substituted by the two direct hydrogen bonds and one water-mediated interaction of the 1, 3-benzodioxole group of inhibitor **1** with Gly 48 (Figure 3B). Importantly, darunavir had no equivalent interaction with the flap residue Gly 48. The interaction of inhibitor **1** with Gly 48 may stabilize the flexible flap region, as observed for the peptide substrates. Both inhibitors share very similar hydrophobic groups and form similar hydrophobic interactions with PR. PR/inhibitor **1** showed slightly more van der Waals interactions between the protein and the inhibitor (100 with distance less than 4.0 Å) than observed for the PR/darunavir complex (96 with distance less than 4.0 Å).

Comparison of Inhibitor Interactions in PR and Mutants. Overall, inhibitor **1** formed similar hydrogen bond interactions in the four mutant complexes and in the wild type PR complex, with the exception of PR_{D30N} (Figure 4). Generally, the mutants showed altered hydrophobic contacts of inhibitor with the mutated residues. The significance of the small structural differences in the mutant complexes relative to wild type PR are best demonstrated in comparison to the changes described for the same mutant complexes with darunavir.[10,11] Both inhibitor **1** and darunavir showed similar hydrogen bond interactions with PR, PR_{V82A}, and PR_{I84V}, while small differences were observed for the other two mutants (Figure 4). The interactions of each mutant will be considered separately.

The complex with PR_{V82A} had a single conformation of inhibitor and Ala 82, whereas Val 82 and inhibitor **1** had two alternate conformations in the other structures. The side chain of Val 82 in the PR/inhibitor **1** structure formed 3 C−H···π interactions with the phenyl group at *P*1 and a van der Waals contact with the *P*1′ group. The interactions of Ala 82 in the mutant are very similar, because the main chain of residue 82 has moved by 0.5 and 0.8 Å for the Cα atoms of the two subunits, respectively, compared to the wild type (Figure 4A,B). This structural change has repositioned the side chain of Ala 82 to form 3 C−H···π interactions with the *P*1 phenyl and one van der Waals interaction with the *P*1′ leucine-like group of inhibitor. A similar shift of Ala 82 compared to Val 82 was observed for the corresponding complexes with darunavir[11] and indinavir.[26]

Reduced van der Waals contacts and loss of a C−H···O interaction were apparent in the PR_{I84V}/inhibitor **1** structure. The side chain of the mutated Val 84 had one interaction with the *P*1 phenyl group, while in the wild type PR/inhibitor **1** complex, Ile 84/84′ had a weak CH···O interaction with a sulfonamide oxygen of inhibitor **1** and three hydrophobic contacts with the phenyl group (Figure 4C). In comparison, Val 84 in the PR_{I84V}/darunavir structure had lost two contacts for both conformations of darunavir.[11] For both inhibitors, the mutant showed fewer interactions than in the wild type enzyme.

The mutant PR_{I50V} showed fewer changes in the interactions with inhibitor **1** than were observed for darunavir. A good

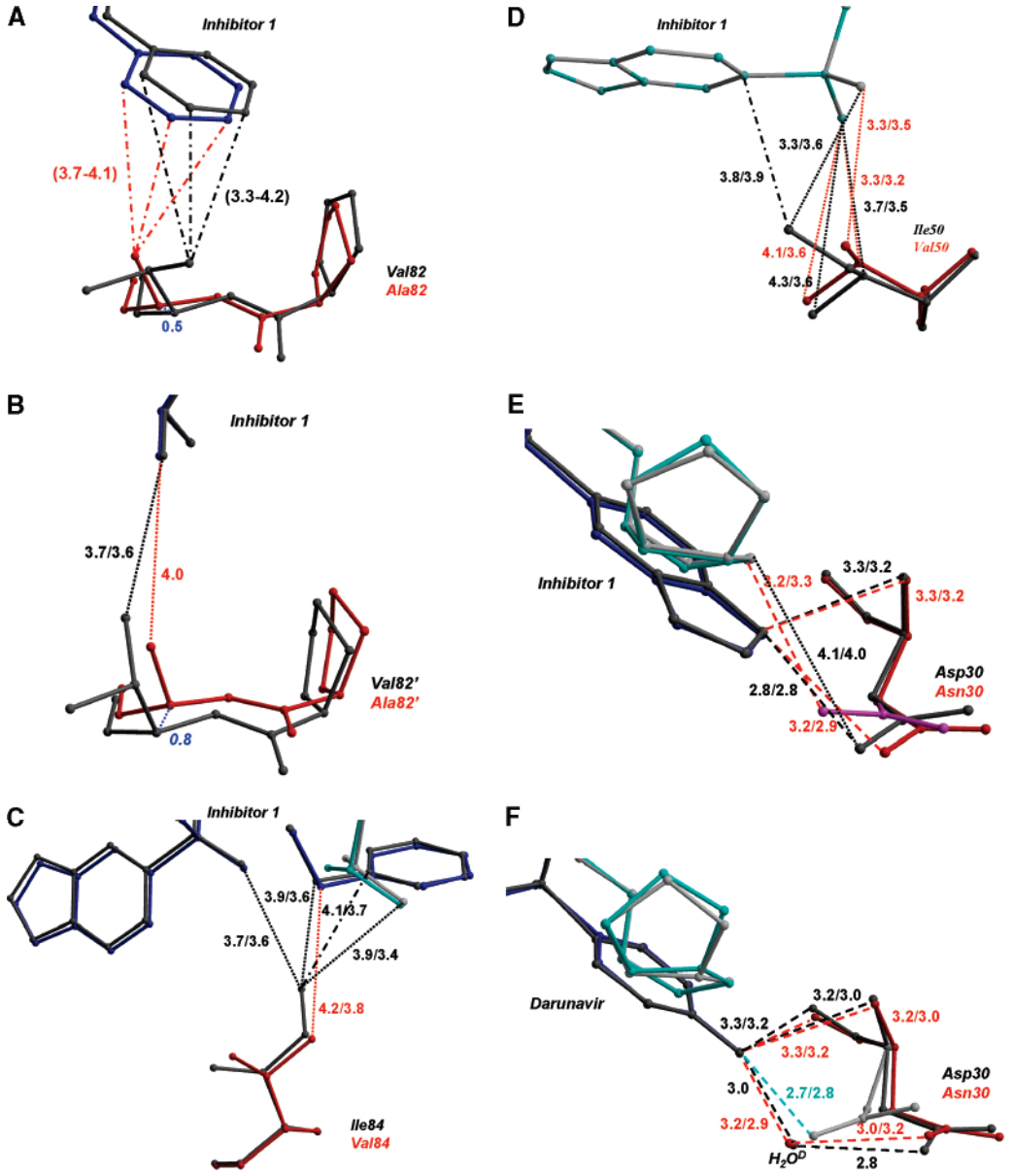

Figure 4. Structural changes in mutants compared to wild type PR. The major and minor conformations of side chains in PR are shown in dark and light gray ball-and-stick, respectively. The alternate conformations in mutant complexes are shown in red and pink, and the alternate conformations of inhibitor are in blue and cyan. The polar interactions are indicated by the dashed lines, van der Waals interactions by the dotted lines, and C−H···π interactions in dot-and-dash line. The interatomic distances are shown in Å for both subunits. (A) Interactions of *P*1 of inhibitor **1** with residue 82 in PR_{V82A} and PR. The minor conformation of inhibitor **1** and alternate conformation of Val82 in PR are omitted for clarity. The shift in position of Cα 82 between PR and mutant is shown in blue dotted lines. (B) Van der Waals interactions of *P*1′ in inhibitor **1** with residue 82′ in PR_{V82A} and PR. View and representation are similar to 4A. (C) PR_{I84V} and PR interactions with inhibitor **1**. (D) PR_{I50V} and PR interactions with inhibitor **1**. Only a single conformation is shown for clarity. (E) PR_{D30N} and PR interactions with inhibitor **1**. (F) PR_{D30N} and PR interactions with darunavir.

hydrophobic C−H···π contact of Ile 50/50′ with the *P*2′ group of inhibitor **1** was lost in the PR_{I50V} mutant (Figure 4D), which is similar to the changes observed in the equivalent complexes with darunavir. The side chain of Val 50 had moved to form a different C−H···O interaction with the sulfonamide oxygen compared to that in the wild type complex. However, inhibitor **1** retained the strong hydrogen bond interactions of the *P*2′ group with Asp 30 in the PR_{I50V} complex, unlike darunavir, where the interaction with the carbonyl oxygen of Asp 30 was absent in the mutant complex.[10] Therefore, darunavir loses a strong hydrogen bond interaction in the PR_{I50V} complex, while inhibitor **1** loses an energetically weaker hydrophobic contact.

The most notable differences were observed in the inhibitor complexes with mutant PR_{D30N} (Figure 4E,F). The structure of PR_{D30N}/darunavir showed a water-mediated interaction of the *P*2′ aniline group with the side chain of Asn 30, instead of the direct hydrogen bond observed for one conformation of Asp 30 in the wild type PR/darunavir structure.[10] In contrast, the polar interactions of the *P*2′ 1,3-benzodioxole group of inhibitor **1** with Asn/Asp 30 were similar in PR_{D30N} and in PR for the major conformations of inhibitor and Asn 30. However, the minor conformation of the Asn 30 side chain formed a new hydrogen bond with an oxygen atom of the bis-THF in the minor conformation of inhibitor **1** (Figure 4E). Therefore, the interactions with inhibitor **1** were maintained in the mutant and wild type PR, while darunavir had replaced a direct hydrogen bond with a water-mediated interaction for one conformation of Asp 30.

The interactions of inhibitor **1** with the mutants may be more similar to those with the wild type PR due to the water-mediated

interaction with Gly 48, which was not seen in the darunavir complexes. This interaction with Gly 48 in the flap will stabilize the closed flap conformation of the protease dimer and more closely mimics the protease interaction with substrates.[27] The absence of a hydrogen bond interaction of darunavir with Gly 48 may facilitate the observed structural changes in its interactions with mutants PR_{D30N} and PR_{I50V}.

Discussion

In preliminary studies, inhibitor **1** has shown extremely potent antiviral activity on HIV-1.[9] Inhibitor **1** showed about 10-fold higher potency for wild type strains of HIV than the chemically related darunavir. Moreover, inhibitor **1** is also chemically related to the protease inhibitor brecanavir, which is in phase III clinical trials.[28] Brecanavir differs from inhibitor **1** in the presence of a large substituted tyrosine at *P*1 instead of the *P*1 phenyl group. The structural and kinetic analyses are reported here for inhibitor **1**, with wild type PR and the drug resistant mutants PR_{D30N}, $PR_{I50V,}$ PR_{V82A}, and PR_{I84V}. The inhibition constants and the protease-inhibitor crystal structures showed relatively small changes compared to the wild type PR, except for PR_{D30N}. Both PR_{D30N} and PR_{V82A} showed compensating interactions with inhibitor **1** relative to those of PR, while reduced hydrophobic contacts were observed with PR_{I50V} and PR_{I84V}. These structural data suggest that inhibitor **1** will maintain inhibitory activity on the resistant variants of HIV containing these mutations. Importantly, inhibitor **1** retained similar polar interactions with PR_{D30N} and PR_{I50V}, unlike the significantly reduced interactions and inhibition of darunavir. Previously, we predicted that darunavir would be less effective on HIV variants containing the D30N or I50V mutations. Our crystallographic, kinetic, and antiviral data suggest that inhibitor **1** will be a valuable addition to the antiviral inhibitors with high potency against resistant strains of HIV. The detailed structural analysis and very similar K_i values for darunavir and inhibitor **1** suggest that the higher antiviral potency of inhibitor **1** arises from better bioavailability and/or better pharmacokinetic behavior.

Experimental Methods

Protein Expression, Purification, and Inhibition Assays. The HIV-1 PR and mutants, which include five mutations Q7K, L33I, L63I, C67A, and C95A to optimize protein stability[29] were constructed, expressed, and purified as described in refs 14, 29−31. Mutations were confirmed by nucleic acid sequencing and protein mass spectrometry.

The inhibition constants were determined by a fluorescence assay using the substrate RE(Edans)SQNY*PIVRK(Dabcyl)R (synthesized by Dr. Ivo Blaha, Ferring Leciva, Prague) as described in ref 18. A total of 8 μL of protease (final concentration of 7−57 nM) was added to a 100 μL solution of 500 mM phosphate buffer, pH = 5.6, 1 M NaCl, 2 mM EDTA, and 10 mM dithiothreitol, and then 2 μL of inhibitor was added. The inhibitors were dissolved in dimethylsulfoxide (DMSO). Their concentrations were determined from peak areas on HPLC (LaChrom, Hitachi, Merck) based on their high structural similarities for amprenavir. The mixture was preincubated at 37 °C for 5 min and 90 μL of substrate dissolved in water (final concentration of 6 μM) was then added to the mixture to initiate the reaction. The reaction solution was assayed over 5 min for the increase in fluorescence using 355 nm excitation and 460 nm emission wavelengths in a Wallac 1420 Victor^2 fluorimeter-luminometer (Wallac Oy, Turku, Finland). Inhibition constants were obtained from the IC_{50} values estimated from a dose−response curve using the equation $K_i = (IC_{50} - 0.5[E])/(1 + [S]/K_m)$, where $[E]$ and $[S]$ are the PR and substrate concentrations, respectively.

Crystallographic Analysis. The inhibitor **1** was dissolved in dimethylsulfoxide (DMSO) and centrifuged briefly to remove any insoluble material. The inhibitor **1** was mixed with protease in a ratio of 2:1 to 5:1. Crystals were grown by the hanging-drop vapor-diffusion method at room temperature. Crystals of the PR_{D30N} complex grew from a 2.5 mg/mL protein solution at pH 4.8 with 25 mM sodium acetate, 10% (w/v) sodium chloride, 0.5% dioxane, and 1.5% (v/v) DMSO. The PR_{I50V} complex crystallized from a 2.3 mg/mL protein solution at pH 4.6 with 25 mM sodium acetate, 9.4% (w/v) sodium chloride, and 6.7% (v/v) DMSO. The PR_{V82A} complex crystallized from a 3.3 mg/mL protein solution at pH 5.0 with 25 mM citrate phosphate, 10% (w/v) sodium chloride, and 6−7% (v/v) DMSO. Crystals of the PR_{I84V} complex grew from a 2.5 mg/mL protein solution buffered at pH 5.0 with 25 mM sodium acetate, 8% (w/v) sodium chloride, and 10% (v/v) DMSO.

A single crystal was mounted in a fiber loop with 20−30% (v/v) glycerol as cryoprotectant in the reservoir solution. X-ray diffraction data were collected at Advanced Photon Source, SER-CAT beamline. The data were integrated, scaled, and merged using the HKL2000 package.[32] The structures were solved by molecular replacement with AMoRe[33] using the starting model 1FS65 from the Protein Data Bank[34] for PR_{V82A} and PR for the other structures. Refinement was carried out using SHELX-97[35] and manual adjustment used the molecular graphics program O.[36] Structural figures were made using Bobscript,[37] Ras3D, and PyMol.[38]

Acknowledgment. Y.T. was supported in part by a Molecular Basis of Disease Fellowship, and I.T.W. and R.W.H. are Distinguished Cancer Scholars. The research was supported in part by the Molecular Basis of Disease Program, the Georgia Research Alliance, the Georgia Cancer Coalition, and the National Institute of Health Grants GM62920 and GM53386. We thank the staff at the SER-CAT beamline at the Advanced Photon Source, Argonne National Laboratory, for assistance during X-ray data collection. Use of the Advanced Photon Source was supported by the U.S. Department of Energy, Office of Science, Office of Basic Energy Sciences, under Contract No. DE-AC02-06CH11357.

References

(1) Barbaro, G.; Lucchini, A.; Barbarini, G. Highly active antiretroviral therapy in HIV-associated pulmonary hypertension. *Minerva Cardioangiol.* **2005**, *53*, 153−154.
(2) Barlett, J. A.; DeMasi, R.; Quinn, J.; Moxham, C.; Rousseau, F. Overview of the effectiveness of triple combination therapy in antiretroviral-naïve HIV-1 infected adults. *AIDS* **2001**, *15*, 1369−1377.
(3) Palella, F. J., Jr.; Delaney, K. M.; Moorman, A. C.; Loveless, M. O.; Fuhrer, J.; Satten, G. A.; Aschman, D. J.; Holmberg, S. D. Declining morbidity and mortality among patients with advanced human immunodeficiency virus infection. HIV outpatient study investigators. *N. Engl. J. Med.* **1998**, *338*, 853−860.
(4) Grabar, S.; Pradier, C.; Le Corfec, E.; Lancar, R.; Allavena, C.; Bentata, M.; Berlureau, P.; Dupont, C.; Fabbro-Peray, P.; Poizot-Martin, I.; Costagliola, D. Factors associated with clinical and virological failure in patients receiving a triple therapy including a protease inhibitor. *Aids* **2000**, *14*, 141−149.
(5) Hertogs, K.; Bloor, S.; Kemp, S. D.; Van den Eynde, C.; Alcorn, T. M.; Pauwels, R.; Van Houtte, M.; Staszewski, S.; Miller, V.; Larder, B. A. Phenotypic and genotypic analysis of clinical HIV-1 isolates reveals extensive protease inhibitor cross-resistance: a survey of over 6000 samples. *AIDS* **2000**, *14*, 1203−1210.
(6) Wu, T. D.; Schiffer, C. A.; Gonzales, M. J.; Taylor, J.; Kantor, R.; Chou, S.; Israelski, D.; Zolopa, A. R.; Fessel, W. J.; Shafer, R. W. Mutation patterns and structural correlates in human immunodeficiency virus type 1 protease following different protease inhibitor treatments. *J. Virol.* **2003**, *77*, 4836−4847.
(7) Rhee, S. Y.; Liu, T.; Ravela, J.; Gonzales, M. J.; Shafer, R. W. Distribution of human immunodeficiency virus type 1 protease and reverse transcriptase mutation patterns in 4183 persons undergoing genotypic resistance testing. *Antimicrob. Agents Chemother.* **2004**, *48*, 3122−3126.
(8) De Clercq, E. New approaches toward anti-HIV chemotherapy. *J. Med. Chem.* **2005**, *48*, 1297−1313.
(9) Ghosh, A. K.; Sridhar, P. R.; Kumaragurubaran, N.; Koh, Y.; Weber, I. T.; Mitsuya, H. Bis-tetrahydrofuran: A privileged ligand for a new generation of HIV-protease inhibitors that combat drug-resistance. *ChemMedChem* **2006**, *1*, 939−950.

(10) Kovalevsky, A. Y.; Tie, Y.; Liu, F.; Boross, P. I.; Wang, Y. F.; Leshchenko, S.; Ghosh, A. K.; Harrison, R. W.; Weber, I. T. Effectiveness of nonpeptide clinical inhibitor TMC-114 on HIV-1 protease with highly drug resistant mutations D30N, I50V, and L90M. *J. Med. Chem.* **2006**, *49*, 1379−1387.
(11) Tie, Y.; Boross, P. I.; Wang, Y. F.; Gaddis, L.; Hussain, A. K.; Leshchenko, S.; Ghosh, A. K.; Louis, J. M.; Harrison, R. W.; Weber, I. T. High resolution crystal structures of HIV-1 protease with a potent nonpeptide inhibitor (UIC-94017) active against multi-drug-resistant clinical strains. *J. Mol. Biol.* **2004**, *338*, 341−352.
(12) Jarvis, B.; Faulds, D.; Nelfinavir, A review of its therapeutic efficacy in HIV infection. *Drugs* **1998**, *56*, 147−167.
(13) Mahalingam, B.; Louis, J. M.; Reed, C. C.; Adomat, J. M.; Krouse, J.; Wang, Y. F.; Harrison, R. W.; Weber, I. T. Structural and kinetic analysis of drug resistant mutants of HIV-1 protease. *Eur. J. Biochem.* **1999**, *263*, 238−245.
(14) Mahalingam, B.; Louis, J. M.; Hung, J.; Harrison, R. W.; Weber, I. T. Structural implications of drug resistant mutants of HIV-1 protease: High resolution crystal structures of the mutant protease/substrate analogue complexes. *Proteins: Struct., Funct., Genet.* **2001**, *43*, 455−464.
(15) Tisdale, M.; Myers, R.; Randall, S.; Maguire, M.; Ait-Khaled, M.; Elston, R.; Snowden, W. Resistance of the HIV protease inhibitor amprenavir in vitro and in clinical studies. *Clin. Drug Invest.* **2000**, *20*, 267−285.
(16) Johnson, V. A.; Brun-Vezinet, F.; Clotet, B.; Kuritzkes, D. R.; Pillay, D.; Schapiro, J. M.; Richman, D. D. Update of the drug resistance mutations in HIV-1: Fall 2006. *Top. HIV Med.* **2006**, *14*, 125−130.
(17) Amano, M.; Koh, Y.; Das, D.; Li, J.; Leschenko, S.; Wang, Y. F.; Boross, P. I.; Weber, I. T.; Ghosh, A. K.; Mitsuya, H. A novel bis-tetrahydrofuranylurethane-containing nonpeptidic protease inhibitor (PI) GRL-98065 potent against multi-PI-resistant HIV in vitro. *Antimicrob. Agents Chemother.* **2007**, *51*, 2143−2155.
(18) Bagossi, P.; Kadas, J.; Miklossy, G.; Boross, P.; Weber, I. T.; Tozser, J. Development of a microtiter plate fluorescent assay for inhibition studies on the HTLV-1 and HIV-1 proteinases. *J. Virol. Methods* **2004**, *119*, 87−93.
(19) Reiling, K. K.; Endres, N. F.; Dauber, D. S.; Craik, C. S.; Stroud, R. M. Anisotropic dynamics of the JE-2147-HIV protease complex: Drug resistance and thermodynamic binding mode examined in a 1.09 A structure. *Biochemistry* **2002**, *41*, 4582−4594.
(20) Nayal, M.; Di Cera, E. Valence screening of water in protein crystals reveals potential Na^+ binding sites. *J. Mol. Biol.* **1996**, *256*, 228−234.
(21) Kovalevsky, A. Y.; Liu, F.; Leshchenko, S.; Ghosh, A. K.; Louis, J. M.; Harrison, R. W.; Weber, I. T. Ultra-high resolution crystal structure of HIV-1 protease mutant reveals two binding sites for clinical inhibitor TMC114. *J. Mol. Biol.* **2006**, *363*, 161−173.
(22) Gustchina, A.; Sansom, C.; Prevost, M.; Richelle, J.; Wodak, S. Y.; Wlodawer, A.; Weber, I. T. Energy calculations and analysis of HIV-1 protease-inhibitor crystal structures. *Protein Eng.* **1994**, *7*, 309−317.
(23) Hodge, C. N.; Aldrich, P. E.; Bacheler, L. T.; Chang, C. H.; Eyermann, C. J.; Garber, S.; Grubb, M.; Jackson, D. A.; Jadhav, P. K.; Korant, B.; Lam, P. Y.; Maurin, M. B.; Meek, J. L.; Otto, M. J.; Rayner, M. M.; Reid, C.; Sharpe, T. R.; Shum, L.; Winslow, D. L.; Erickson-Viitanen, S. Improved cyclic urea inhibitors of the HIV-1 protease: Synthesis, potency, resistance profile, human pharmacokinetics, and X-ray crystal structure of DMP 450. *Chem. Biol.* **1996**, *3*, 301−314.
(24) Lam, P. Y.; Jadhav, P. K.; Eyermann, C. J.; Hodge, C. N.; Ru, Y.; Bacheler, L. T.; Meek, J. L.; Otto, M. J.; Rayner, M. M.; Wong, Y. N.; et al. Rational design of potent, bioavailable, nonpeptide cyclic ureas as HIV protease inhibitors. *Science* **1994**, *263*, 380−384.
(25) Lam, P. Y.; Ru, Y.; Jadhav, P. K.; Aldrich, P. E.; DeLucca, G. V.; Eyermann, C. J.; Chang, C. H.; Emmett, G.; Holler, E. R.; Daneker, W. F.; Li, L.; Confalone, P. N.; McHugh, R. J.; Han, Q.; Li, R.; Markwalder, J. A.; Seitz, S. P.; Sharpe, T. R.; Bacheler, L. T.; Rayner, M. M.; Klabe, R. M.; Shum, L.; Winslow, D. L.; Kornhauser, D. M.; Hodge, C. N.; et al. Cyclic HIV protease inhibitors: Synthesis, conformational analysis, *P*2/*P*2′ structure−activity relationship, and molecular recognition of cyclic ureas. *J. Med. Chem.* **1996**, *39*, 3514−3525.
(26) Mahalingam, B.; Wang, Y. F.; Boross, P. I.; Tozser, J.; Louis, J. M.; Harrison, R. W.; Weber, I. T. Crystal structures of HIV protease V82A and L90M mutants reveal changes in the indinavir-binding site. *Eur. J. Biochem.* **2004**, *271*, 1516−1524.
(27) Tie, Y.; Boross, P. I.; Wang, Y. F.; Gaddis, L.; Liu, F.; Chen, X.; Tozser, J.; Harrison, R. W.; Weber, I. T. Molecular basis for substrate recognition and drug resistance from 1.1 to 1.6 angstroms resolution crystal structures of HIV-1 protease mutants with substrate analogs. *FEBS J.* **2005**, *272*, 5265−5277.
(28) Ford, S. L.; Reddy, Y. S.; Anderson, M. T.; Murray, S. C.; Fernandez, P.; Stein, D. S.; Johnson, M. A. Single-dose safety and pharmacokinetics of brecanavir, a novel human immunodeficiency virus protease inhibitor. *Antimicrob. Agents Chemother.* **2006**, *50*, 2201−2206.
(29) Wondrak, E. M.; Louis, J. M. Influence of flanking sequences on the dimer stability of human immunodeficiency virus type 1 protease. *Biochemistry* **1996**, *35*, 12957−12962.
(30) Wlodawer, A.; Erickson, J. W. Structure-based inhibitors of HIV-1 protease. *Annu. Rev. Biochem.* **1993**, *62*, 543−585.
(31) Louis, J. M.; Wondrak, E. M.; Copeland, T. D.; Smith, C. A.; Mora, P. T.; Oroszlan, S. Chemical synthesis and expression of the HIV-1 protease gene in *E. coli*. *Biochem. Biophys. Res. Commun.* **1989**, *159*, 87−94.
(32) Otwinowski, Z.; Minor, W. Processing of X-ray diffraction data in oscillation mode. *Methods Enzymol.* **1997**, *276*, 307−326.
(33) Navaza, J. AMoRe: An automated package for molecular replacement. *Acta Crystallogr., Sect. A: Found. Crystallogr.* **1994**, *A50*, 157−163.
(34) Berman, H. M.; Westbrook, J.; Feng, Z.; Gilliland, G.; Bhat, T. N.; Weissig, H.; Shindyalov, I. N.; Bourne, P. E. The Protein Data Bank. *Nucleic Acids Res.* **2000**, *28*, 235−242.
(35) Sheldrick, G. M.; Schneider, T. R. SHELXL: High resolution refinement. *Methods Enzymol.* **1997**, *277*, 319−343.
(36) Jones, T. A.; Zou, J. Y.; Cowan, S. W.; Kjeldgaard, M. Improved methods for building protein models in electron density maps and the location of errors in these models. *Acta Crystallogr., Sect. A: Found. Crystallogr.* **1991**, *A47*, 110−119.
(37) Esnouf, R. M. Further additions to MolScript version 1.4, including reading and contouring of electron-density maps. *Acta Crystallogr., Sect. D: Biol. Crystallogr.* **1999**, *55*, 938−940.
(38) DeLano, W. L. *The PyMOL Molecular Graphics System*; DeLano Scientific: San Carlos, CA, 2002.

JM070482Q